JARO 19: 493–510 (2018)
DOI: 10.1007/s10162-018-0680-x

Research Article

JARO
Journal of the Association for Research in Otolaryngology

Reflection- and Distortion-Source Otoacoustic Emissions: Evidence for Increased Irregularity in the Human Cochlea During Aging

Carolina Abdala,[1] Amanda J. Ortmann,[1] and Christopher A. Shera[1]

[1]*Auditory Research Center, Caruso Department of Otolaryngology, University of Southern California, 1640 Marengo Street, Suite 346, Los Angeles, CA 90033, USA*

Received: 8 March 2018; Accepted: 1 June 2018; Online publication: 2 July 2018

ABSTRACT

Previous research on distortion product otoacoustic emission (DPOAE) components has hinted at possible differences in the effect of aging on the two basic types of OAEs: those generated by a reflection mechanism in the cochlea and those created by nonlinear distortion (Abdala and Dhar in J Assoc Res Otolaryngol 13:403–421, 2012). This initial work led to the hypothesis that micromechanical irregularity ("roughness") increases in the aging cochlea, perhaps as the result of natural tissue degradation. Increased roughness would boost the backscattering of traveling waves (i.e., reflection emissions) while minimally impacting DPOAEs. To study the relational effect of aging on both types of emissions and address our hypothesis of its origin, we measured reflection- and distortion-type OAEs in 77 human subjects aged 18–76 years. The stimulus-frequency OAE (SFOAE), a reflection emission, and the distortion component of the DPOAE, a nonlinear distortion emission, were recorded at multiple stimulus levels across a four-octave range in all ears. Although the levels of both OAE types decreased with age, the rate of decline in OAE level was consistently greater for DPOAEs than for SFOAEs; that is, SFOAEs are relatively preserved with advancing age. Multiple regression analyses and other controls indicate that aging per se, and not hearing loss, drives this effect. Furthermore, SFOAE generation was simulated using computational modeling to explore the origin of this result. Increasing the amount of mechanical irregularity with age produced an enhancement of SFOAE levels, providing support for the hypothesis that increased intra-cochlear roughness during aging may preserve SFOAE levels. The characteristic aging effect—relatively preserved reflection-emission levels combined with more markedly reduced distortion-emission levels—indicates that SFOAE magnitudes in elderly individuals depend on more than simply the gain of the cochlear amplifier. This relative pattern of OAE decline with age may provide a diagnostic marker for aging-related changes in the cochlea.

Keywords: SFOAE, DPOAE, aging roughness, emission

INTRODUCTION

Otoacoustic emissions (OAEs) are low-level sounds generated by active and nonlinear cochlear processes. These sounds provide a window into cochlear mechanics and hold promise for providing a deeper understanding of sensory hearing loss. Two basic classes of otoacoustic emissions have been defined: linear reflection and nonlinear distortion. These two OAE types do not map onto cochlear properties in the same way. This is not surprising given that they arise from distinct intra-cochlear generation processes (Shera and Guinan 1999). Reflection-source emis-

Present address: Amanda J. Ortmann, Department of Otolaryngology, Washington University School of Medicine, 660 S. Euclid Ave, Campus Box 8042, St. Louis, MO 63110, USA.
Correspondence to: Carolina Abdala · Auditory Research Center, Caruso Department of Otolaryngology · University of Southern California · 1640 Marengo Street, Suite 346, Los Angeles, CA 90033, USA. Telephone: 626-673-2213; email: carolina.abdala@usc.edu

sions, such as the click-evoked OAE or stimulus-frequency OAE (SFOAE), are thought to arise from coherent backscattering of wavelets off of fixed micromechanical irregularities distributed along the cochlear partition (Zweig and Shera 1995). By contrast, distortion-source emissions, such as the distortion-product OAE (DPOAE), are generated by cochlear nonlinearities associated with sensory hair cell transduction.

Reflection- and distortion-source OAEs can be independently affected by experimental variables such as salicylates, activation of the medial efferent reflexes, development, aging, and genetic mutations (Abdala et al. 2009; Deeter et al. 2009; Abdala and Dhar 2010, 2012; Rao and Long 2011; Cheatham et al. 2016). Examining both reflection and distortion emissions in the same ear during aging will help us understand how factors important for the generation of these distinct OAEs change during the human lifespan. The findings may also have important implications for the clinical application of OAEs to the aging population.

There is ample literature examining the general decline of DPOAE magnitude with aging, often complicated by associated changes in hearing (e.g., Lonsbury-Martin et al. 1991; Stover and Norton 1993; Castor et al. 1994; Dorn et al. 1998; Uchida et al. 2008; Hoth et al. 2010; Ortmann and Abdala 2016). Although the present study contributes to this copious literature, its focus is to examine the *relationship* between these two classes of emissions during aging, so as to better understand the course of cochlear function and its degradation during senescence. Work from our laboratory studying the unmixed reflection and distortion components of the DPOAE introduced the notion that these two distinct components are not equally degraded by the aging process (Abdala and Dhar 2012). Although this paradigm is experimentally convenient, the separated reflection and distortion components are not independent emissions: The reflection component arises from the distortion via scattering of the distortion wave near its tonotopic place. Also, although there are signal processing techniques to separate components of the DPOAE, the separation is imperfect (Abdala et al. 2016); the SNR of the reflection component, which contributes a relatively small portion of the total DPOAE under most commonly used protocols, is typically low, and one cannot quantify and control probe strength to the reflection site. Hence, unmixing the total DPOAE is not the optimal way to characterize the relationship between these two OAE types.

Despite this limitation, the initial study discovered an intriguing pattern. As expected, the magnitudes of both the reflection and distortion components of the DPOAE declined with age. However, although the distortion component of the DPOAE in elderly subjects was reduced in level relative to other age groups (including newborns, infants, teens, and young adults), reflection-component levels were more similar among age groups. Additionally, we found that the fine structure of the DPOAE increased with advancing age, showing deeper peaks and valleys and more numerous oscillations (see also Poling et al. 2014). In common DPOAE protocols, the distortion component dominates the total DPOAE. Enhanced fine structure suggests that the contribution of the two components comprising the total DPOAE becomes more equal with aging, thereby producing a more prominent interference pattern. Although the equivalence of component levels can be achieved in various ways, it suggests that the relationship between the two components is changing with age.

To explain this finding, we hypothesized that the aging ear may have increased micromechanical irregularity or "roughness" associated with natural tissue degradation. Increased roughness could augment the backscattering of waves launched along the cochlea by providing additional reflection points, cumulatively producing a larger reflection emission despite other deleterious effects of aging, such as the loss of cochlear gain (i.e., diminished hearing sensitivity).

In this study, we investigate the changing relationship between distortion and reflection emissions during aging using two independent emission measures in every ear: the stimulus frequency OAE, representing the class of reflection emissions, and the distortion component of the DPOAE, representing the class of nonlinear distortion emissions. In addition, we explore our hypothesis that aging-related increases in cochlear roughness can explain the relative preservation of reflection-source OAEs in the aging ear using OAE simulations.

METHODS

Subjects

Subjects included 77 adults: 20 young adults (13F; mean age = 22.3 years; range 18–31 years), 25 middle-aged adults (18F; mean age = 51 years; range = 40–60 years), and 32 older adults (27F; mean age = 68 years; range = 62–76 years). There was a preponderance of female subjects in the older groups (19M, 58F); although the sex distribution is not ideal, we were constrained by the pool of elderly subjects volunteering for our study. In each age group, 13 of the tested ears were right ears. Prior to inclusion, an audiogram was conducted in 2-dB steps from 0.5 to 8 kHz at half-octave and octave intervals. Potential subjects were excluded if they had hearing loss below 2 kHz or greater than 55 dB HL at any frequency above 2 kHz. Figure 1 provides the mean audiometric thresholds for each age group ±1 SD. Although the

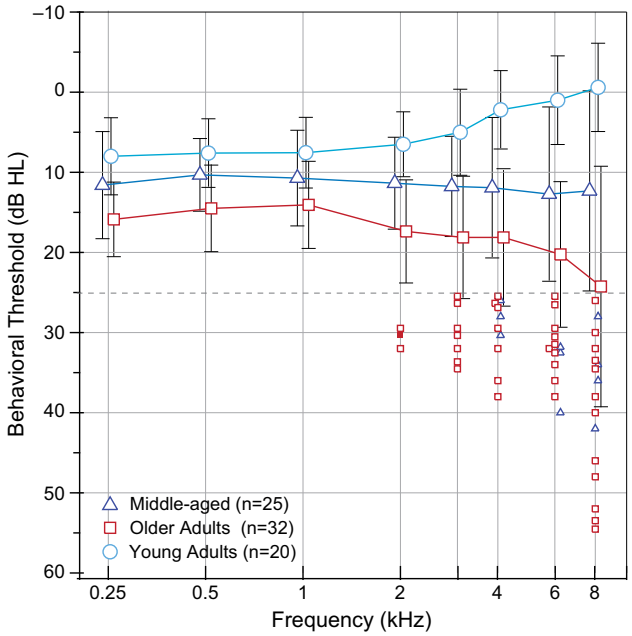

FIG. 1. Mean audiogram (± 1 SD) for each of three age groups: young-adult, middle-aged adult, and older adult. The middle-aged and older-adult groups had some thresholds that fell outside of the range conventionally considered normal (i.e., 25 dB HL) although well within what is considered "normal" for their respective ages. The elevated thresholds are displayed as small individual symbols

mean values for the three age groups fall within the audiometrically normal range, individual subjects from the older groups had elevated thresholds above 2 kHz, which is considered typical for this age range (see Morrell et al. 1996). Individual thresholds exceeding 25 dB HL are indicated by small symbols.

Subjects were screened for middle-ear disease in two ways: (1) When air-conduction thresholds exceeded 20 dB HL, a corresponding bone-conduction threshold was obtained. Individuals with an air–bone gap >10 dB (indicative of middle ear involvement) were not accepted into the study, and (2) standard tympanometry with a 226-Hz probe tone was conducted. Subjects were required to have peak compliance at pressure values between +/- 50 daPa. Mean tympanometric peak compliance was noted at +18, +15, and +18 daPa for young, middle-aged, and older adults, respectively. In addition to these two screening tests to establish normal middle-ear function, ear-canal energy reflectance (ratio of reflected to incident energy in the ear canal) from 0.25 to 8 kHz was measured in all subjects and did not differ significantly among age groups.

Instrumentation, Signal Processing, and Parameters

Stimulus generation and OAE acquisition were controlled using a custom-developed MATLAB-based swept-tone algorithm via a Babyface USB 2.0 High Speed Audio Interface (RME Audio, Germany) and an Etymotic Research ER-10C probe system. Subjects were tested within a double-walled IAC sound booth while seated or reclining in an ergonomic chair and watching a subtitled video or just resting. The ER-10C probe cable was suspended from the ceiling of the sound booth and coupled to the ear with a nylon strap around the forehead of each participant.

Stimulus-Frequency OAEs. Stimuli were swept tones whose instantaneous frequency changed smoothly and linearly (in a downward direction) at rate of 2 kHz/s. Four individual frequency segments, each spanning 1.8 kHz, were presented concurrently as a stack. Recent work has shown that there is little difference in SFOAE amplitude or phase between a single sweep SFOAE and one generated with concurrent sweeping, so long as the starting frequencies of each segment are separated by between 0.6 and 1 octave (Abdala et al. 2018). The advantage of the four-segment concurrent sweeping method is that data collection time is reduced by a factor of four relative to the time required for a single continuous frequency sweep.

Stimulus-frequency OAEs were measured using an interleaved suppression paradigm (Shera and Guinan 1999). Four intervals were presented: p_1 = probe tone alone, p_2 = suppressor tone (+ polarity) and probe, p_3 = probe tone alone, and p_4 = suppressor tone (− polarity) and probe. The SFOAE waveform is calculated as $p_{sf} = (p_1 + p_3)/2 - (p_2 + p_4)/2$, which results in two SFOAE measurements for each block of four intervals. SFOAE probe tones were swept from 0.5 to 8 kHz and presented at three probe levels: 40 dB SPL in all subjects, young and old; 20 dB SPL in young adults; and, because not all older participants had measureable responses at 20 dB SPL, 30 dB SPL in middle-aged and older adults. Suppressor tones were swept simultaneously with the probe tone at a frequency 50 Hz below the probe frequency at 55 dB SPL. Between 64 and 512 sweeps were presented and averaged to produce an SFOAE estimate; greater numbers of sweeps were presented at the lower probe levels.

Multiple internal reflections occur when outgoing SFOAE waves reflect from the stapes footplate back into the cochlea; the reflected waves peak at the probe frequency site and are re-reflected basal-ward, contributing as a component of the SFOAE measured in the ear canal. These repeated internal reflections can contaminate estimates of OAE delay. To focus on the primary reflection at the probe frequency, analyses of SFOAEs have implemented various signal processing methods to eliminate longer-latency contributions (e.g., Konrad-Martin and Keefe 2005; Shera and Bergevin 2012; Mishra and Biswal 2016; Abdala et al. 2018). Here, we applied a time-domain filtering

technique (inverse FFT, or IFFT) to window the main reflection of the SFOAE while eliminating probe/suppressor contamination and longer-latency energy associated with multiple cochlear reflections.

For the IFFT analysis, SFOAE data were resampled with 12-Hz frequency resolution. Overlapping (50 Hz overlap) Hann-windowed segments of the SFOAE were transformed into the pseudo-time domain. The time-domain windows were centered around the mean of published SFOAE delay curves (Shera et al. 2002), $\tau(f)$, which varies with frequency according to a power-law function from 14.4 ms at the lowest frequency to 3 ms at the highest. The time windows were banded by the curves $0.5\tau(f)$ on the short-latency end (τ_{short}) and $1.5\tau(f)$ on the long-latency end (τ_{long}), consistent with the work of Moleti et al. (2012). The windowed data were then transformed back into the frequency domain using the FFT. The noise was passed through the same time-domain filter as the SFOAEs and served as a reference for signal-to-noise (SNR) calculations.

Distortion-Product OAEs. Distortion-product OAEs at $2f_1–f_2$ were measured with pairs of primary tones logarithmically swept upwards from 0.5 to 8 kHz at 0.5 octaves/s with a fixed f_2/f_1 ratio of 1.22. A full input/output function was generated by recording the DPOAE from 25 to 80 dB SPL with primary tones presented in 5-dB step size, using the "scissors" approach to determine primary-tone level separation ($L_1 = 0.4L_2 + 39$; Kummer et al. 1998). Only the *distortion component* of the DPOAE was analyzed in this study for comparison with the SFOAE. The distortion component was isolated by combining a long analysis window (500 ms) with a relatively rapid sweep rate (0.5 octaves/s), which effectively eliminates the longer-latency reflection elements (Long et al. 2008; Abdala et al. 2015). Henceforth, whenever the acronym DPOAE is used without qualification in this report, it refers to the separated distortion component of the total DPOAE. We applied phase-rotation averaging to cancel the primary tones during measurement of the total DPOAE (Whitehead et al. 1996); three stimulus intervals with different starting phases were interleaved such that f_1 and f_2 were canceled and only the emission remained once the block was averaged. For young-adult subjects, 24 sweeps were presented across the test frequency range; for middle- and older-adult subjects, 24 sweeps were presented for $L_2 > 50$ dB SPL and 48 sweeps for $L_2 \leq 50$ dB SPL.

Stimulus Calibration. To mitigate the effect of ear-canal standing waves on stimulus level, calibrated stimuli were delivered to each subject after compensating for the depth of probe insertion (Lee et al. 2012). The half-wave resonance was recorded in the ear of each subject and used to select a matched pressure response previously recorded (at various insertion depths) in an ear simulator (IEC 60318-4; BK 4157). The matched pressure response in the coupler was used to compensate the frequency response of the sound sources and approximate a relatively flat response across frequency at the tympanic membrane. As a measure of probe stability, we monitored the half-wave resonance peak in the ear canal every 12 min throughout the test session.

Least Squares Fit Analysis. SFOAE and DPOAE levels and phases were estimated using a least squares fitting (LSF) technique (Long et al. 2008; Kalluri and Shera 2013; Abdala et al. 2015). To apply LSF modeling, the time waveform recorded at the microphone is segmented into analysis windows. Models for the probe, suppressor, and the OAE are created and the signals of interest within each analysis window were then estimated by a least squares fit, which minimizes the sum of the squared residuals between the model and the data to achieve the best fit. DPOAEs and SFOAEs evoked with swept tones and analyzed with an LSF technique produce estimates of amplitude and phase that are comparable to those generated with discrete tones (Long et al. 2008; Kalluri and Shera 2013; Abdala et al. 2015, 2018).

For both emission types, the noise floor was estimated by taking the difference between adjacent sweep pairs and applying the LSF to this difference. System distortion was calculated by running the OAE protocol in a coupler (IEC 60318-4; BK 4157). For SFOAEs, system distortion ranged from −45 to −21 dB SPL, with an overall mean level of −29 dB SPL across frequency and level. For DPOAEs, distortion levels ranged from −40 to −21 dB SPL, with an overall mean level of −30 dB SPL. The system distortion was lower than (or in a few conditions, equal to) biological noise floors measured in the ear canal of each subject; therefore, they were unlikely to influence estimates of OAE level.

Protocol

Data collection was conducted in two test sessions, each lasting 2–3 h with breaks taken as needed. The test ear was selected as the ear with the better-combined OAE SNR and audiometric thresholds. Because this study sought to define changes in the *relationship* between SFOAE and DPOAEs in the same ear, selecting appropriate comparison levels was important. These two distinct OAEs have different dynamic ranges and input/output characteristics (Schairer et al. 2003; Ortmann and Abdala 2016; Abdala and Kalluri 2017; Abdala et al. 2018). Although both SFOAE and DPOAE levels grow with increasing stimulus level and then saturate, the stimulus level at which this plateau occurs, termed here the compression threshold, is different for the

SFOAE and DPOAE. In general, SFOAE levels saturate at lower stimulus levels than DPOAE levels by roughly 8–10 dB (Abdala and Kalluri 2017). For this reason, we studied the relationship between SFOAEs and DPOAEs both at stimulus levels fixed with regard to the approximate compression threshold of each emission and also, more conventionally, at a fixed sound pressure level. OAE compression thresholds were derived from mean DPOAE and SFOAE input/output (I/O) functions collected in previous studies from our laboratory using the same methodology. In those studies, the compression threshold was estimated with a fit to the I/O function (see Ortmann and Abdala 2016 for DPOAEs and Abdala et al. 2018 for SFOAEs). OAE I/O functions measured from older adults show response compression at stimulus levels that are approximately 6–8 dB higher than those observed in young adults (Ortmann and Abdala 2016; Ortmann et al. 2017); these age-related adjustments were also incorporated in the SFOAE–DPOAE comparisons.

The DPOAE and SFOAE comparisons in this study were conducted at three levels: (1) a low stimulus level (LSL), in which both OAEs were measured below their respective compression thresholds in the growing portion of their input/output functions. For the LSL comparison in young adults, SFOAEs at 20 dB SPL were compared to DPOAEs generated with an L_2 of 30 dB SPL; for middle- and older-adult subjects, SFOAEs at 30 dB SPL were compared to DPOAEs generated at an L_2 of 40 dB SPL. (2) A high stimulus level (HSL), in which both emissions were measured at or just above their compression thresholds in the compressed region of their input/output functions. For the HSL comparison, SFOAEs at a probe level of 40 dB SPL were compared to DPOAEs at an L_2 of 50 dB SPL for all ages. (3) A fixed stimulus level (FSL) in which both OAEs were measured at the same fixed level (probe and $L_2 = 40$ dB SPL).

Analysis

Subjects (and conditions) with non-measurable emissions were removed from the database prior to analysis. Pre-IFFT SFOAE levels and corresponding noise floors were averaged within 10, third-octave frequency bands with center frequencies ranging from 786 to 6288 Hz. Frequency bands with an average SNR less than 6 dB were eliminated, and subjects or conditions with more than five (of 10) eliminated frequency bands were entirely removed from the database. At 40 dB SPL, three older-adult female subjects were removed; at 30 dB SPL, seven older-adult female subjects and two middle-aged subjects, one male and one female, were removed; and at 20 dB SPL (a level at which only young-adult data were analyzed), one young-adult male subject was removed.

Basic SFOAE level, phase, and delay group trends were generated for the three age groups to describe how aging impacts SFOAEs, which has not previously been reported. Both descriptive statistics and analyses of variance were applied for this purpose and all the data are presented without any averaging so as to show their sometimes idiosyncratic nature. To examine the *relationship* between the two emissions, OAE level was averaged into half-octave frequency bands denoted by center frequency. Scatter plots of OAE level versus age were generated and regression lines fit separately to the SFOAEs and DPOAEs. The slope of the regression line indicates the rate of decline of OAE level with age and was calculated for all level and frequency conditions. Level differences (dB) were also calculated in each ear at each center frequency as SFOAE level minus DPOAE level, and a regression line was fit to these difference values. To test whether the difference slopes were non-zero and significant (i.e., indicative of a changing relationship between SFOAE and DPOAE levels across age), we resampled the data using Monte Carlo permutation tests in which the ages were randomly shuffled. A p value of 0.05 was considered significant. Multiple regression tests were also conducted on this level difference value considering both age and hearing loss as factors.

RESULTS

Aging Effects on SFOAE Level

Unlike DPOAEs, changes in the SFOAE with aging have not previously been described. Therefore, we first report basic aging analyses for the SFOAE; comparable analyses are not shown for the DPOAE given the existing literature in this area. Figure 2 presents SFOAE spectra measured at 20 and 40 dB SPL for young adults, and 30 and 40 dB SPL for middle-aged and older adults. No SNR criteria were applied to the SFOAEs in this figure; all data are shown. While the variability of SFOAE level among ears (thin lines) is great due to each ear's idiosyncratic SFOAE spectral structure, a feature intrinsic to reflection emissions, a loess trend line fit to the spectra allows one to visualize the group trends.

The young-adult group shows mean SFOAE levels for a 40 dB SPL probe ranging from 2 to 8 dB SPL below 2 kHz with strongest levels at frequency bands centered at 786 and 1247 Hz. Above 2 kHz, mean SFOAE levels decrease rapidly. At 40 dB SPL, both middle-aged and older-adult groups also show peak SFOAE levels below 2 kHz. Interestingly, the peak is shifted slightly toward higher frequencies in the older-adult group, as evidenced by the trend lines in the bottom panels of Fig. 2. The inset in Fig. 2 shows the level trend lines for the three age groups

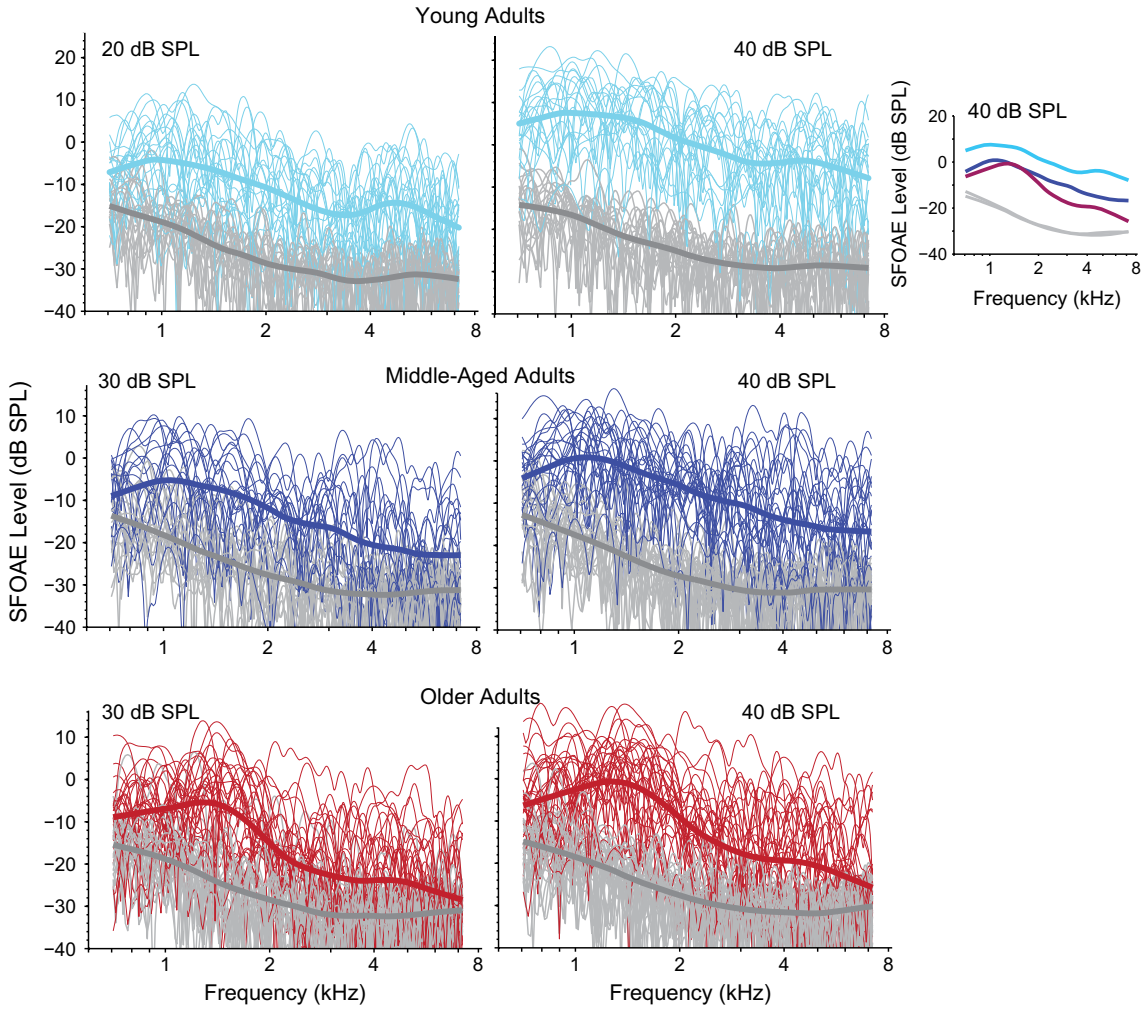

FIG. 2. The SFOAE amplitude spectra of all subjects are displayed in three age groups at two probe levels (the lower level condition is 20 dB SPL for young-adults and 30 dB SPL for middle-aged and older adults). The young-adult data are cyan, the middle-aged adults are royal blue and the older-adult data are shown in red while the noise floor is shown in gray. A loess trend line was fit to group data to help visualize the age trends. Loess lines (for SFOAE the 40 dB SPL probe condition) are superimposed in the inset figure without individual data

superimposed at 40 dB SPL. Age differences are most apparent at the higher frequencies.

The SFOAE evoked at the lower stimulus levels retains the same basic spectral shape for all three groups but amplitude drops considerably. For young adults, at 20 dB SPL, mean SFOAE levels range from 0 to −15 dB SPL across frequency. This marked drop suggests a steep decline in SFOAE magnitude with decreasing stimulus level and is consistent with the near-linear slope observed in the SFOAE input/output functions (Schairer et al. 2003; Abdala and Kalluri 2017; Abdala et al. 2018).

Aging Effects on SFOAE Phase and Delay

Although changes in DPOAE phase with aging have been characterized in previous work (Abdala and Dhar 2012), the effects of aging on SFOAE phase and group delay have not been described in the literature. Figure 3 plots SFOAE phase-versus-frequency functions and loess trend lines at 40 dB SPL for the three age groups; the inset shows the trend lines superimposed. For all ages, the SFOAE shows the rapid phase rotation that characterizes reflection-source emissions. The two older groups show nearly indistinguishable phase functions, which are steeper overall than those measured in young adults. Phase accumulation was indexed by subtracting starting phase (at the lowest frequency) from ending phase (at the highest frequency), and this metric was tested with an ANOVA for age effects. Mean accumulation for young adults was 31.7 cycles and 35.3 cycles for middle-aged and older-adult subjects. A

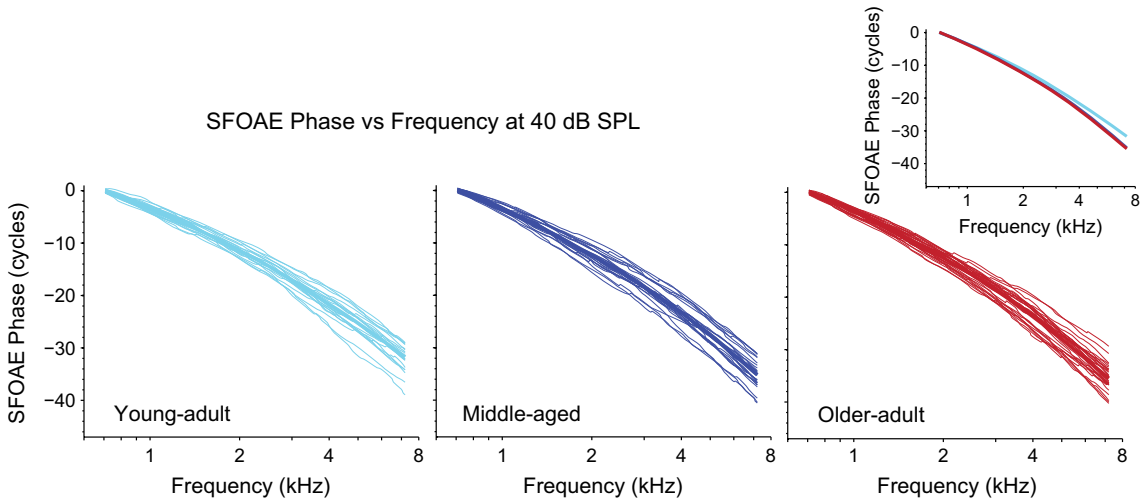

FIG. 3. SFOAE phase versus frequency functions (measured at a probe level of 40 dB SPL) are plotted for each individual ear in three age groups. The young-adult data are shown in cyan, the middle-aged group in royal blue and the older-adult data in red. A loess trend line is fit to the data in each group. The smaller inset shows the group trends lines superimposed without individual data

one-way ANOVA showed an age effect on phase accumulation ($F = 35.47$; $p = 0.0001$): both middle-aged and older-adult groups had greater accumulation (consistent with overall steeper phase slope) than the young-adult group.

The SFOAE phase data were converted to group delay by calculating the negative of the slope of the phase as $\tau(f) = -\mathrm{d}\phi_{\mathrm{SFOAE}}(f)/\mathrm{d}f$, where $\phi_{\mathrm{SFOAE}}(f)$ is SFOAE phase in cycles. Following the convention of Shera and Guinan (2003), SFOAE delays were then expressed in dimensionless form as the equivalent number of periods of the stimulus frequency: $N_{\mathrm{SFOAE}}(f) = f \cdot \tau(f)$. Figure 4 shows loess trend lines (and their 95% confidences intervals) fit to the individual N_{SFOAE} data points from three age groups. The loess line was fit only to group delay values from spectral peaks of the SFOAE to best elucidate the underlying delay trend (Shera and Bergevin 2012). Across much of the frequency range, the trend line

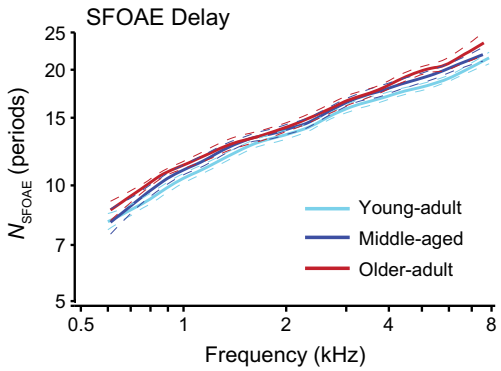

FIG. 4. Loess trend lines fit to individual normalized SFOAE delay, N_{SFOAE}, plotted as a function of frequency for each age group. The young-adult data is in cyan, the middle-aged in royal blue, and the older-adult data is shown in red. 95 % confidence intervals for the fit are also displayed as dashed lines

indicates that the two older groups have slightly longer delays than those of the young adults. This finding is consistent with the greater phase accumulation and steeper phase gradient in older adults. We speculate on possible reasons for this interesting age difference in the "Discussion" section.

The Relationship Between SFOAE and DPOAEs During Aging

SFOAE Versus DPOAE Level. The primary goal of this study is to understand changes in the *relationship* between reflection (SFOAE) and distortion (DPOAE) emissions during aging. To this end, Fig. 5 provides a preliminary look at trend lines fit to group SFOAE and DPOAE levels across frequency for the three age groups in the low-stimulus-level condition (i.e., where both OAEs are measured in the low-level, growing portion of their own input/output function—see "Methods" section for definitions of each level comparison condition). In these data, mean DPOAE levels are generally higher than SFOAE levels, and both OAEs decrease with advancing age (moving from top to bottom panel), most notably in the high frequencies. However, the two emissions are not equally affected by aging. The gap between the SFOAE and DPOAE level trend lines reduces progressively between panels, suggesting that the rate of decline differs for the two emissions: DPOAE levels appear to decrease more rapidly with age than do SFOAE levels. Data in the high-stimulus-level condition (i.e., both OAEs measured in the compressed region of the input/output function) and the fixed-stimulus-level (40 dB SPL) comparison condition show a similar pattern, indicating that the relationship between OAEs changes with aging.

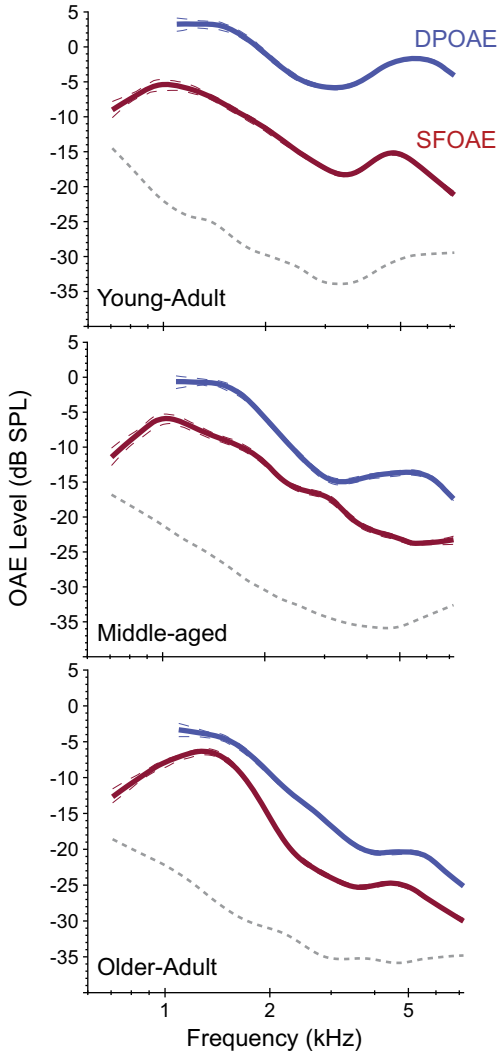

FIG. 5. Loess trend lines that were fit to individual amplitude spectra for each age group and both OAE types are shown for the low-stimulus-level condition. As one moves from top to bottom panel, the gap between SFOAE and DPOAE amplitude trends narrow, indicating a changing relationship between reflection and distortion OAE level with aging

To examine this effect, age was un-grouped and plotted as a continuous variable on the *x*-axis of a scatter plot while OAE level was plotted on the *y*-axis. This was done independently for each of five half-octave frequency bands denoted by their center frequencies: 1303, 1843, 2607, 3702, and 5202 Hz. The left panels of Fig. 6 are scatterplots of SFOAE (red) and DPOAE (blue) levels as a function of age for one representative frequency band centered at 1843 Hz in two level conditions: low- and fixed-stimulus levels. Each point has an error bar derived from the SNR in dB. In particular, the error bar (in dB) is given by $\mathrm{dB}(1+1/\mathrm{adB}(\mathrm{SNR}))$, where the function $\mathrm{dB}(x) \equiv 20\log_{10}(x)$ and $\mathrm{adB}(x)$ inverts the conversion to dB, so that $\mathrm{adB}(\mathrm{dB}(x)) = x$. With this definition, the error bar is 6 dB at 0 dB SNR and vanishes as the SNR approaches infinity. Linear regression lines were fit to the DPOAE and SFOAE level data separately to assess the rate of OAE decline as a function of age for each emission. Regression lines generally had a negative slope indicating reductions in OAE level with age for both emissions, though the decline was less at the lower frequencies. Figure 7 displays the mean slopes (dB/year) derived from the regression lines fit to SFOAE and DPOAE level versus age plots at the five frequency bands for the low- and fixed-stimulus levels. The error bars represent ±1 SD and were estimated using a resampling procedure (over the target half-octave band) that takes into account the uncertainty of each individual data point. In all cases, the slope of the SFOAE decline with aging is shallower than that of the DPOAE.

A level difference score was calculated for the pair of measurements in each ear [SFOAE level minus DPOAE level (in dB)] and plotted as a function of age. A linear regression was fit to the difference data shown in the right-hand panels of Fig. 6 for one center frequency. In young adulthood, most level difference values are negative, indicating that the DPOAE is higher in level than the SFOAE, but with advancing age the level difference crosses zero around early middle age (where the two OAEs are equal in level). Values then become slightly positive during senescence, indicating that the SFOAE has become the relatively stronger OAE. These data appear to conflict with Fig. 5, where the DPOAE remains the higher-level response throughout the age range; however, the effect is due to analysis and display differences between the two figures. Here, we have averaged frequency into half-octave bands and consider age as a continuum, which elucidates different trends than do the data in Fig. 5.

A Monte Carlo resampling procedure with random reshuffling of age was performed to test whether the slopes of the regression lines fit to the SFOAE–DPOAE level difference versus age data were significantly different from zero, which would indicate a shifting relationship during aging. Slopes were significant for four frequency bands in the low-stimulus-level comparison condition (1303 Hz, $p = 0.001$; 1843 Hz, $p = 0.000$; 3702 Hz, $p = 0.001$; 5202 Hz, $p = 0.0006$) and borderline for one (2607 Hz, $p = 0.07$). The linear fits account for up to 23% of the variance. (R^2 range from 0.05 to 0.23; R^2 of 0.05 was noted for 2607 Hz, which showed the least variance accounted for in all conditions.) For the fixed-stimulus-level comparison condition, all five frequency bands show significant slopes for the difference level versus age data (p values range from $p = 0.0001$ to $p = 0.049$) and the fits account for up to 24% of the variance (R^2 ranged from 0.05 to 0.24). In the high-stimulus-level comparison condition, three frequency bands (1303,

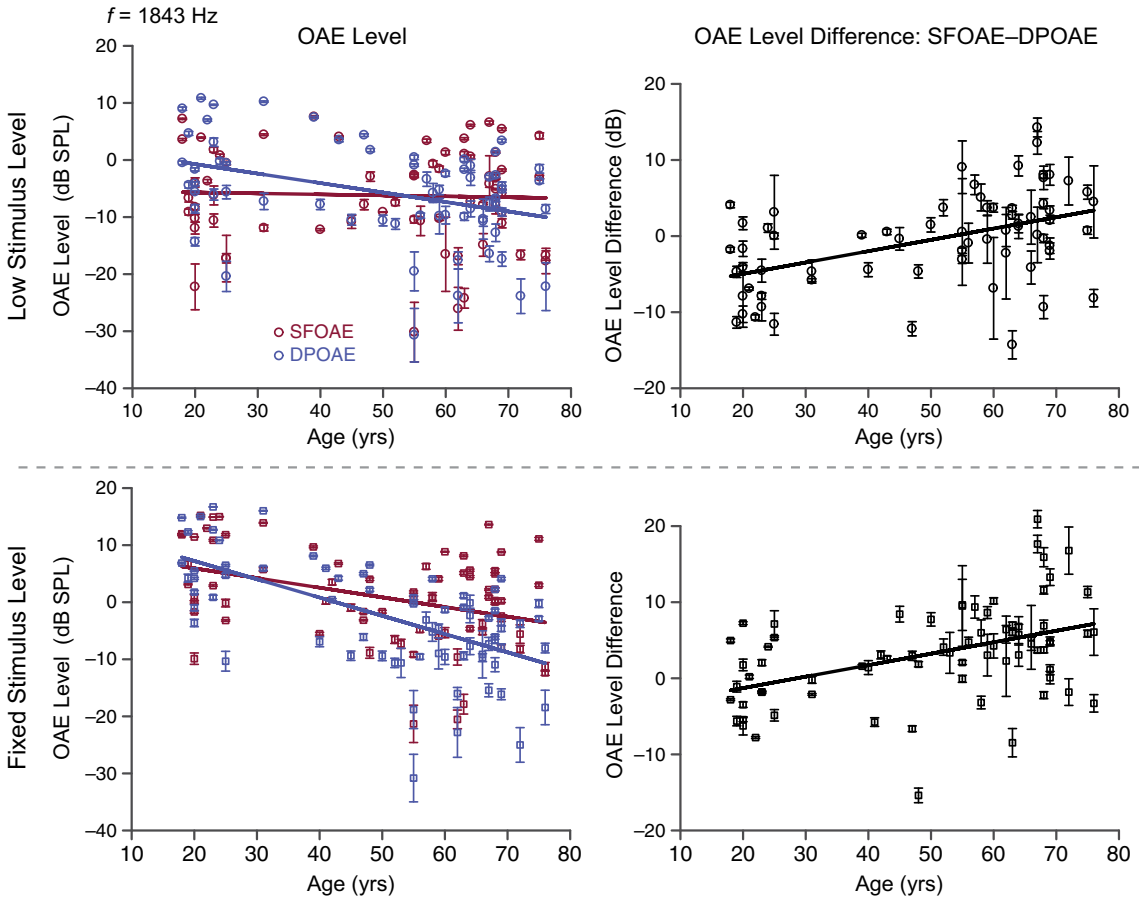

FIG. 6. SFOAE (red) and DPOAE (blue) level values are plotted as a function of age. Here, the data are displayed for one center frequency, 1843 Hz, and two level conditions: low- and fixed-stimulus levels. Each data point includes error bars reflecting the uncertainty in the measurement of the estimate over the targeted half-octave band. A linear regression line fit separately to the SFOAE and DPOAE level data was always negative, indicating reductions in the level of both OAEs with age; however, the slope of DPOAE decline with age was steeper than that observed for SFOAE data. The panels in the right column show SFOAE–DPOAE level differences versus age and the linear regression lines fit to these difference scores. Data below 0 dB indicate the DPOAE is higher in level than SFOAE; points above 0 dB indicate that the SFOAE has become the relatively higher-level response with aging.

1843, and 3202 Hz) show significant slopes ($p < 0.001$, 0.006, and 0.047, respectively).

This analysis confirms that the relationship between the two OAEs changes with age—in particular, SFOAE levels decrease less than DPOAE levels with advancing age. Because the two lower-level conditions are more sensitive to the aging effect and produce comparable results, we focus solely on the fixed stimulus level condition in subsequent comparisons.

The Confounding Effect of Hearing Loss. The characteristic pattern of relative SFOAE and DPOAE level decline with age is robustly present at multiple stimulus frequencies and levels; however, interpreting the pattern as a result of aging per se requires accounting for possible confounds, the most obvious of which is hearing loss. The process of aging is strongly correlated with the deterioration of hearing (Fitzgibbons and Gordon-Salant 2010), and our subjects show age-related differences in their audiometric thresholds (see Fig. 1). Furthermore, the characteristic aging pattern we detect—relatively preserved SFOAE levels—is also apparent when we consider OAE levels as a function of hearing threshold. We plotted SFOAE and DPOAE levels as a function of audiometric threshold (HL) at roughly matched frequencies (OAE at 1303 Hz matched with HL at 1000 Hz, OAE at 1843 Hz with HL at 2000 Hz, OAE at 2607 Hz with HL at 3000 Hz, OAE at 3702 Hz with HL at 4000 Hz, and OAE at 5202 Hz OAE with HL at 6000 Hz) and computed the mean slopes of the regression lines fit to these data (see Fig. 8). DPOAE slope approaches 1 dB/dB at some mid-to-high frequencies where the correlation between DPOAE level and hearing threshold is particularly strong and accounts for 60–70% of the variance. SFOAE levels also decrease with increasing audiometric threshold but are more weakly correlated with hearing, showing shallower slopes than the DPOAE. These data raise

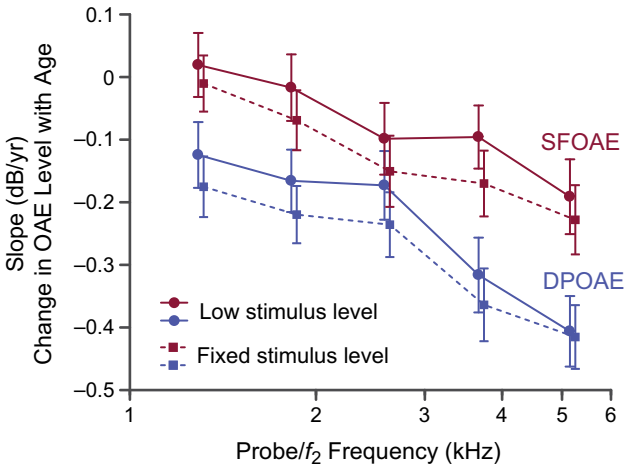

FIG. 7. The slope values (dB/year) derived from linear regression fits to SFOAE (red) and DPOAE (blue) level are shown as a function of the five center frequencies ranging from 1303 to 5202 Hz. The error bars represent ± 1 standard deviation computed by resampling while considering the individual uncertainty in each point on the OAE level × age scatter plots over the targeted half-octave band. The slopes are presented for two comparison le= vels: low- (solid) and fixed-stimulus levels (dashed lines). The DPOAE slopes (reflecting the decline of OAE level with age) are steeper than those of the SFOAE at all frequencies

the question whether our characteristic pattern of OAE decline is primarily a consequence of aging or of hearing loss (or both).

We addressed this confound in two ways. First, we conducted multiple regression analyses on the SFOAE–DPOAE level difference, including both age and audiometric threshold as factors. Five regression analyses were conducted, one at each center frequency, in the fixed-stimulus-level condition. The fits

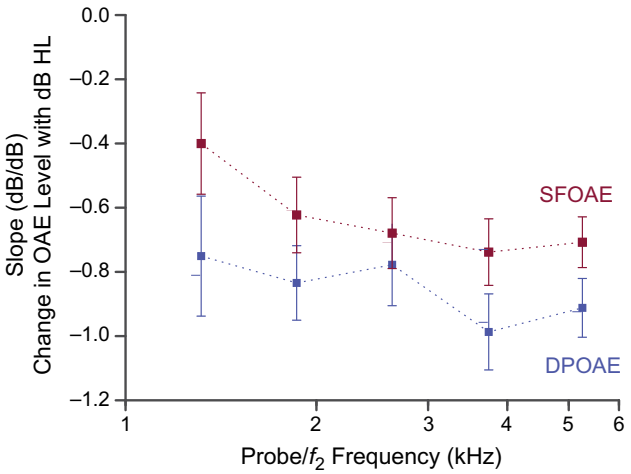

FIG. 8. The slope values derived from linear regression fits to SFOAE and DPOAE levels versus audiometric thresholds at roughly corresponding frequencies. The error bars represent ± 1 standard deviation computed by resampling while considering the individual uncertainty in each point over the targeted half-octave band. DPOAE levels correlate to audiometric thresholds better than the SFOAE levels and show a nearly linear relationship to hearing in the high-frequencies. The characteristic pattern of relative SFOAE preservation (shallower slope of decline) is observed as a function of hearing

captured up to 24% of the variance across frequency; at four of the five frequencies, the slopes were significant for the aging factor ($p = 0.00003$, 0.00003, 0.09, 0.01, 0.01) but not for audiometric threshold.

Second, we culled our original aging database of 57 middle-aged and older-adult subjects (some of whom showed elevated audiometric thresholds) down to the 31 ears with hearing thresholds in the normal range (≤ 20 dB HL). The audiometric pure tone average or PTA (mean of hearing thresholds at 0.5, 1, and 2 kHz) from this subset of middle-aged/older group matched the young-adult group to within 4 dB. The top panel of Fig. 9 shows a linear regression fit to SFOAE and DPOAE level versus age for the subset of *normal hearers only* at one example frequency (1843 Hz) in the fixed-stimulus-level condition. Although subjects with clinically significant hearing loss have been removed from the analysis, a steeper decline in level (with regard to SFOAE) is still observed for the DPOAEs with advancing age. All frequency and level conditions

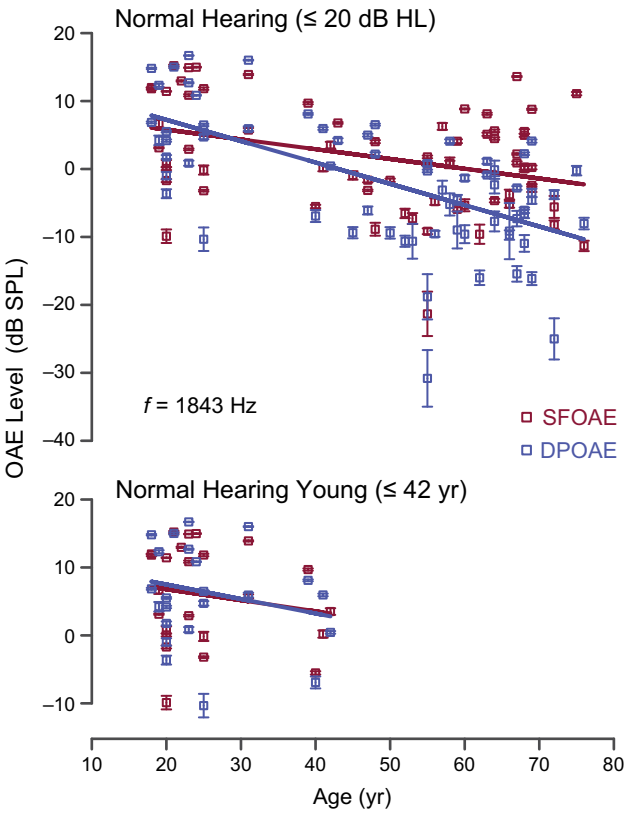

FIG. 9. In this figure, the middle-aged and older-aged subjects are restricted to a subset of subjects with normal hearing, < 20 dB HL. The top panel shows a linear regression fit to SFOAE (red) and DPOAE (blue) levels as a function of age at one center frequency, 1843 Hz only (fixed stimulus level condition). The characteristic pattern of steeper DPOAE than SFOAE decline is still present even though data from all ears with hearing loss have been eliminated. The bottom panel further culls these data by including only "young" normal-hearers defined as those younger than 42 years of age at one example frequency, 1843 Hz. When aging is eliminated as a variable, the SFOAE and DPOAE level decline as a function of age becomes comparable

produced this same pattern. Evidently, hearing loss (defined here as thresholds > 20 dB HL) does not drive the observed relationship between SFOAE and DPOAE level as a function of age. Threshold variations below 20 dB HL could have contributed to the SFOAE–DPOAE pattern of level decline; however, this is not likely given that average audiometric thresholds were matched to within 4 dB for the young and middle-/older-aged adults in this subset.

We also culled our original dataset in one other way: we eliminated "aging" (as distinct from numerical age) from the analysis. For convenience, and considering our spread of data points, we considered the variable of aging at play for any subject over the age of 42 years. We reasoned that if aging is the dominant contributor to the signature pattern of SFOAE level preservation observed, then the slopes of SFOAE and DPOAE regression lines should become more similar once aging was eliminated. The results shown in the bottom panel of Fig. 9 for one frequency are consistent with this prediction; the SFOAE and DPOAE regression lines are almost superimposed. This outcome applies across frequency as illustrated in Fig. 10, which plots the mean slopes of fits to OAE level versus age for the young normal-hearing group. When aging is eliminated, SFOAE and DPOAE decline with age become nearly equivalent. Regression slopes (dB/year) derived from the level differences (SFOAE–DPOAE) in this young subset are not significantly different from zero.

We conclude that even when hearing threshold is considered and controlled (to the extent possible in our data), aging produces a differential effect on DPOAE and SFOAE levels. Furthermore, aging appears to be the necessary and sufficient factor producing this characteristic pattern of OAE decline.

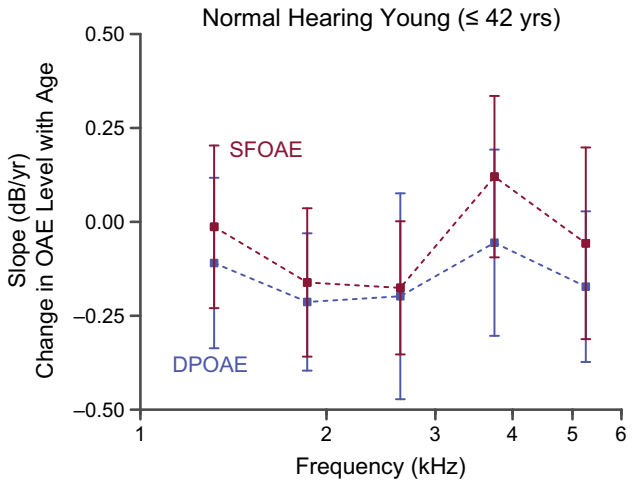

FIG. 10. The slopes (dB/year) derived from the regression fits to young, normal-hearing ears only are shown as a function of five center frequencies for SFOAEs (red) and DPOAEs (blue) in the fixed-stimulus-level condition. When aging is eliminated by restricting data to young normal-hearing ears, the rates of OAE level decline with age become more similar and equivalent at some frequencies. The characteristic pattern is weakened and almost eliminated as noted by the reduced gaps between the red and blue lines

OAE Simulations and Modeling

To explore whether aging-related increases in cochlear irregularity can partially offset what would otherwise be a more pronounced (i.e., DPOAE-like) decline in SFOAE levels with aging, we simulated SFOAEs using a simple, phenomenological model of SFOAE generation (Shera and Bergevin 2012). The simulations allow independent manipulation of relevant parameters, including the amount and pattern of mechanical irregularity as well as the gain, group delay, and frequency tuning of the auditory filter (equivalently, the gain, wavelength, and spatial spread of the traveling wave peak). We examined the effect of parameter variations on SFOAE levels to test the hypothesis that increasing roughness during aging can explain the relative preservation of SFOAE level with age.

As detailed below, we simulated SFOAEs from 74 "ears" with 200 points/octave resolution over half-octave-wide frequency intervals centered on our five principal analysis frequencies (1.3, 1.8, 2.6, 3, 7, and 5.2 kHz). Traveling-wave gain at each frequency was estimated from the subject's hearing level (HL) and the overall dependence of DPOAE level on HL (i.e., changes in DPOAE level were used to estimate effective changes in cochlear gain). Group delays and tuning bandwidths (i.e., ERBs) were set to match mean values appropriate for the subject's age (see data in Fig. 4 for N_{SFOAE} and Hopkins and Moore 2011 for ERBs in aging subjects). Irregularity patterns were constructed using random numbers drawn from a zero-mean Gaussian distribution. The roughness magnitude (standard deviation of the Gaussian distribution) was either held constant or varied with age.

Model Description. When multiple internal reflection within the cochlea can be neglected (e.g., after time-frequency filtering of the OAE), the model emission pressure has the form (Shera 2003):

$$\hat{P}_{SFOAE} = P_0 G_{ME} R, \quad (1)$$

where $P_0(f)$ is the stimulus source pressure, $G_{ME}(f)$ characterizes round-trip middle-ear transmission, and $R(f)$ is the cochlear reflectance, representing the complex amplitude of the reverse-traveling wave (normalized by the ingoing wave) at the stapes. We describe the production of reverse-traveling waves within the cochlea using an equation borrowed from the coherent-reflection model of reflection-source OAE generation (Shera et al. 2005, 2008):

$$R(f) \sim \int \varepsilon(x)\ W^2(x, f)\ dx, \quad (2)$$

where $\varepsilon(x)$ represents the micromechanical irregularity and $W(x,f)$ is a weighting function summarizing membrane–fluid coupling and round-trip pressure-difference wave propagation between the stapes and the site of scattering at cochlear position x. Although the integration extends throughout the cochlea, its value is dominated by the peak region of the traveling wave. Near the peak, located at $\hat{x}(f)$, we approximate $W(x,f)$ by a Gaussian envelope and a locally linear phase, a phenomenological description previously used to capture the essential features of the coherent-reflection model (Zweig and Shera 1995; Talmadge et al. 2000):

$$W(x,f) = \widehat{W} e^{-[(x-\hat{x})/2\Delta x]^2} e^{-2\pi i(x-\hat{x})/\hat{\lambda}}. \quad (3)$$

The parameters $\hat{\lambda}$ and Δx determine, respectively, the local wavelength and spatial spread of the traveling-wave envelope.

To approximate the variation in tuning, wavelength, and delay believed characteristic of the human cochlea (e.g., Shera and Guinan 2003), we allow the model parameters to vary with location (or equivalently with the local characteristic frequency, which we take to vary exponentially with position, $\mathrm{CF}(x) = \mathrm{CF}(0)e^{-x/\ell}$, with $\hat{x}(f)$ satisfying $\mathrm{CF}(\hat{x}(f)) = f$, and where ℓ is the space constant of the tonotopic map; in humans, $\mathrm{CF}(0) \approx 20$ kHz and $\ell \approx 7.2$ mm; Greenwood 1990). Specifically, for the wavelength, we take $\hat{\lambda}(\mathrm{CF}) = \ell / N_W(\mathrm{CF})$, where $N_W(\mathrm{CF}) = N_1(\mathrm{CF}/\mathrm{kHz})^{\gamma}$, with $\gamma = 0.6$ for $\mathrm{CF} < \mathrm{CF_{a|b}}$ and $\gamma = 0.37$ for $\mathrm{CF} > \mathrm{CF_{a|b}}$ (Shera and Bergevin 2012; Shera and Guinan 2003). The apical–basal transition CF was approximated as $\mathrm{CF_{a|b}} = 1$ kHz (Shera et al. 2010). In practice, we eliminate the discontinuity in γ by changing its value smoothly over a span of a few hundred Hertz. For the spatial spread of the wave, we take $\Delta x = \ell / \sqrt{2\pi} Q_{\mathrm{ERB}}$, with $Q_{\mathrm{ERB}}(\mathrm{CF}) = Q_1(\mathrm{CF}/\mathrm{kHz})^{0.3}$ (Shera et al. 2002). As discussed below [near Eqs. (5) and (6)], the parameters N_1 and Q_1 are determined from the empirical variation of N_{SFOAE} and Q_{ERB} with age.

Computations of the reflectance using the integral in Eq. (2) were performed numerically by partitioning the cochlea into 3500 longitudinal segments. Since we were not interested in absolute emission levels, we took $G_{\mathrm{ME}} = 1$ and exploited the linearity of the model to adjust the amplitude P_0 to yield a maximum mean emission level of approximately 5 dB SPL in the youngest ears. With the exception of those discussed below, all model parameters were fixed across subjects.

Emission spectra were computed for 74 "ears" (i.e., one per subject) with model parameters adjusted to capture frequency-specific audiometric data from the individual subjects. For subject number n (with $n = 1, 2, \ldots, 74$), the model parameter $\hat{W}(f_i)$ representing the effective traveling-wave "gain" at frequency f_i was estimated from the DPOAE data using the formula

$$\widehat{W}_n^2(f_i) = \mathrm{adB}\big(s_{\mathrm{DPOAE}}(f_i)\ \mathrm{HL}_n(f_i)\big). \quad (4)$$

In this equation, $\mathrm{HL}_n(f_i)$ is the hearing level for the nth subject at frequency f_i estimated by interpolation from the audiogram. The slope $s_{\mathrm{DPOAE}}(f_i)$ has units of dB SPL/dB HL and represents the slope of the empirical regression line relating DPOAE level $[L_{\mathrm{DPOAE}}(f_i)]$ to $\mathrm{HL}(f_i)$, as computed from the data pooled across subjects. The function $\mathrm{adB}(x) \equiv 10^{x/20}$ inverts the conversion to dB. Thus, the model uses measured changes in DPOAE level to estimate effective changes in cochlear gain; in effect, the model assumes that if cochlear gain were the only factor influencing SFOAEs, then SFOAE and DPOAE levels would decline at the same rate with increasing HL.

The parameter $N_1(f_i)$ was varied to capture the empirical dependence of SFOAE delay on age shown in Fig. 4. Specifically, we took

$$N_{1,n}(f_i) = \frac{1}{2}\left(11 + m_{N_{\mathrm{SFOAE}}}(f_i)\ (\mathrm{Age}_n - 20\mathrm{years})\right), \quad (5)$$

where $m_{N_{\mathrm{SFOAE}}}(f_i)$ has units of periods/year and represents the slope of the regression line relating $N_{\mathrm{SFOAE}}(f_i)$ —the SFOAE delay in periods, averaged in half-octave bands about f_i —to subject age.

The parameter $Q_1(f_i)$ was varied to approximate the empirical dependence of the ERB on hearing threshold (Hopkins and Moore 2011). At each of the three frequencies assessed by Hopkins and Moore (0.5, 1, and 2 kHz), the ERB data were converted to Q_{ERB} and their dependence on HL then approximated by a simple function chosen to capture the major trends in the data (sharp tuning in subjects with good thresholds becoming broader with increasing HL). More specifically, the parameters $\hat{Q}_{\mathrm{max}}$ and the slope s_Q were determined at each of the three frequencies by fitting the data to two intersecting straight lines of the form

$$\widehat{Q}_{\mathrm{ERB}} = \begin{cases} \widehat{Q}_{\mathrm{max}} & \mathrm{HL} < 5\mathrm{dB} \\ \widehat{Q}_{\mathrm{max}}\left[1 + s_Q(\mathrm{HL} - 5\ \mathrm{dB})\right] & \mathrm{HL} > 5\ \mathrm{dB}, \end{cases} \quad (6)$$

where the slope s_Q has units of 1/dB HL. The model parameter $Q_1(f_i)$ was then set according to $Q_{1,n}(f_i) = 11\ [1 + s_Q(\mathrm{HL}_n(f_i) - 5\ \mathrm{dB})]$, where we used the value of the slope s_Q obtained from the ERB data closest to f_i.

Finally, the irregularity function $\varepsilon(x)$ was taken to have the form $\varepsilon_n(x) = \varepsilon_0(f_i) r_n(x)$ where $r_n(x)$ is zero-

mean, unit-variance Guassian spatial noise, which we varied randomly from subject to subject. To model changes in "roughness" with age, we took

$$\varepsilon_{0,n}(f_i) = 0.05 \text{ adB}\left[m_\varepsilon(f_i)\ (\text{Age}_n - 20 \text{ years})\right]. \quad (7)$$

In this equation, the parameter $m_\varepsilon(f_i)$ has units of dB/year. Varying its value allows us to determine whether changing the roughness amplitude with age can help "preserve" SFOAE levels (relative to simulations performed with $m_\varepsilon = 0$). Values of all parameters are given in Table 1.

Simulation Results. Figure 11 shows example simulated SFOAEs from an individual ear and how they vary with changes in the parameters that control tuning bandwidth and roughness magnitude (Q_1 and ε_0, respectively). As expected from the linear dependence evident in Eqs. (1) and (2) for $\hat{P}_{\text{SFOAE}}(f)$, SFOAE magnitudes vary in direct proportion to roughness; doubling the value of ε_0 increases SFOAE levels by 6 dB. The dependence on tuning bandwidth (i.e., on the effective width of the scattering region) is more complicated. Doubling the bandwidth (halving Q_1) broadens the region of coherent reflection and generally produces a small increase in SFOAE level and a pronounced smoothing of the spectrum. However, both increases and decreases in SFOAE level are possible, especially near spectral notches. Changes in the parameter N_1 similar to the changes in N_{SFOAE} seen with age (see Fig. 4) affect the emission phase-gradient delay but produce negligible effect on SFOAE levels (not shown).

Figure 12 shows the resulting mean slopes (in dB/year) relating simulated SFOAE levels to age across all "ears". The error bars represent standard deviations of the slopes estimated by resampling. The simulated SFOAE levels generally decrease with age (slope < 0) at a rate that increases with frequency. When the roughness magnitude is held constant (open squares), these changes in SFOAE level are driven primarily by the age- and frequency-related decreases in traveling-wave gain (i.e., increases in hearing thresholds). The broadening of the auditory filters and changes in group delay that accompany these decreases in gain have relatively minor effects on simulated SFOAE level. (By itself, the broadening of the traveling-wave envelope actually enhances SFOAE levels somewhat by increasing the spatial extent of the region of coherent scattering.) Increasing the roughness magnitude systematically with age (black squares) partially compensates for the decrease in gain. By rendering the slopes shallower (closer to zero), the increase in irregularity helps rescue the simulated SFOAE levels, mimicking the observed difference between the decline in SFOAE and DPOAE levels with age. The simulations indicate that increasing the roughness over the six-decade age range of our measurements by a factor of 2–4, depending on frequency, produces a relative increase in SFOAE levels comparable to the differences observed between SFOAEs and DPOAEs. Indeed, because realistic variations in the other model parameters with age have a minor effect on SFOAE levels, the values of the parameter $m_\varepsilon(f_i)$ needed to produce the results in Figure 12 are well approximated by the slopes of the regression lines relating the difference between SFOAE and DPOAEs levels $[L_{\text{SFOAE}}(f_i) - L_{\text{DPOAE}}(f_i)]$ to subject age.

Summary of Results

We have defined some of the basic characteristics of SFOAEs from young-adulthood through senescence. This description provides normative familiarity with the SFOAE during aging, something wholly absent from the literature. Our motivating interest, however, was in studying the effect of aging on the *relationship* between SFOAEs and DPOAEs, which are generated by distinct intra-cochlear processes. Our primary finding is that although aging decreases the levels of both DPOAEs and SFOAEs, *aging has a more marked effect on the level of the distortion-source emission than on the reflection-source emission.* Thus, SFOAE levels are relatively preserved during aging. Although worsening

TABLE 1

Parameter values used in the SFOAE simulations as a function of center frequency, f_i (first row)

f_i (kHz)	1.303	1.843	2.607	3.702	5.202
s_{DPOAE} (dB/dB)	−0.75	−0.83	−0.78	−0.99	−0.91
$m_{N_{\text{SFOAE}}}$ (periods/year)	0.04	0.02	0.02	0.04	0.06
s_Q 1/dB HL	−0.07	−0.1	−0.1	−0.1	−0.1
m_ϵ (dB/year)	0.16	0.15	0.09	0.19	0.19

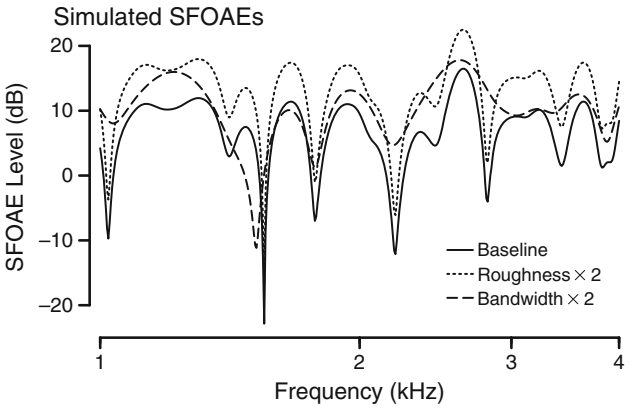

FIG. 11. Simulated SFOAE levels versus frequency and their variation with changes in the parameters Q_1 and ϵ_0 that control tuning bandwidth and roughness magnitude. The roughness patterns $r(x)$ were held constant across the three simulations. Baseline values of the parameters: $Q_1 = 10$ and $\epsilon_0 = 0.05$

hearing thresholds contribute to the general decline in OAE level, they do not explain the differential effect of aging on SFOAE versus DPOAE levels. An additional, unidentified factor—independent of hearing threshold but associated with aging—is affecting relative OAE levels. OAE simulations suggest that augmented irregularity in the aging cochlea can help sustain SFOAE levels, making increased roughness a plausible candidate for this additional factor.

DISCUSSION

There are two basic mechanisms by which otoacoustic emissions arise in the ear: linear reflection and nonlinear distortion. This study sought to probe the relationship between reflection and distortion-source

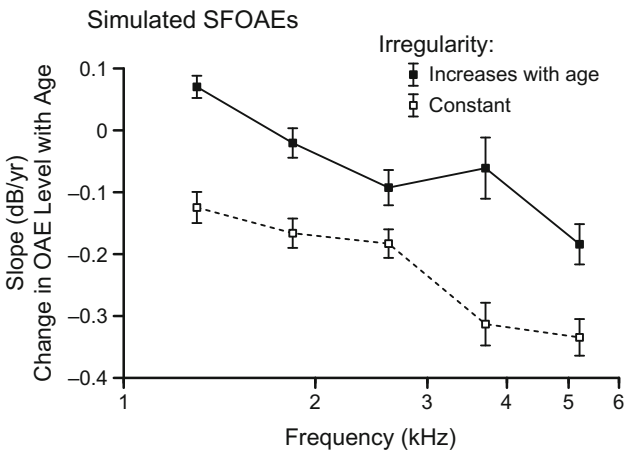

FIG. 12. Regression slopes relating simulated SFOAE levels to age (dB/year) at each of the five center frequencies. Open symbols show slopes computed from simulations in which the roughness magnitude was held constant; solid symbols show that increasing the irregularity with age by a factor of 2.5 partially compensates for the age-related reduction in traveling-wave gain. Error bars give standard deviations computed by resampling

emissions measured in the same ear of subjects whose age spanned six decades. Others have measured both reflection OAEs (in the form of click- or transient-evoked emissions) and DPOAEs during aging (e.g. Castor et al. 1994; Satoh et al. 1998; Hoth et al. 2010). These studies found a general decline in OAE level with age, though the largest of them, with over 5000 subjects (Hoth et al. 2010), attributed most of this decline to hearing loss. These studies concluded that declines in TEOAEs and DPOAEs with aging were correlated and generally similar, but none quantified the effect with a relational metric. Our study, too, found a general decline of SFOAE and DPOAE levels with aging and with hearing loss. Interestingly, Hoth and colleagues provide the slope of OAE decline for both TEOAEs and DPOAEs (see their Table 1), which appears to agree with our findings: DPOAEs show steeper decline in all conditions than TEOAEs. Nevertheless, these early studies recorded relatively simple TEOAE measures and an unseparated DPOAE which included both nonlinear distortion and reflection components. It is difficult to make direct comparisons with the current study.

The signature effect we observed—relative preservation of SFOAE levels with aging—could only have been detected via *comparison* with DPOAE data. Given the expected associations with hearing level, there is little unusual about a decline in either SFOAE or DPOAE level with age. The noteworthy finding is that relative SFOAE and DPOAE levels change with age in a way that appears independent of hearing threshold. These results support the idea that a combined reflection–distortion OAE protocol provides a deeper and more informative probe of sensory hearing loss than either emission used alone. Together with other recent results from our laboratory (Abdala and Kalluri 2017), these findings illustrate the power of using a joint-OAE protocol to detect and understand hearing loss.

The relational nature of the metric becomes important in ruling out the contribution of spurious factors to the findings. For example, subject sex is known to affect OAE level and patterns of presbycusis. However, because each subject served as their own control (i.e., both OAEs came from the same ear for any paired or relational measure), sex effects were minimized or eliminated. Our subject pool included more female than male subjects; hence, we cannot rule out the possibility that relative SFOAE preservation and any increased roughness during aging are restricted to females. We consider this unlikely. Aging effects on middle-ear function also have the potential to confound the results but, again, due to the relational nature of the metric, this is unlikely. Additionally, wideband reflectance measures suggest that no significant differences in middle-ear function

existed among age groups. One might argue that because middle-ear function affects three relevant tones (f_1, f_2, and DP) during DPOAE measurement and only one (the probe) during SFOAE measures, it could produce a differential effect on SFOAEs versus DPOAEs. However, since OAE level was binned into half-octave frequency bands for analysis, any slight frequency differences like this were smeared out and the potential effect minimized.

Aging and SFOAEs

The present study establishes that SFOAEs can be recorded in humans well into their seventh decade of life despite mild amounts of threshold elevation at some frequencies. Not unexpectedly, SFOAE levels and SNRs decline with age, most notably at the high frequencies and lowest probe levels; nevertheless, all but three older-adult subjects had measureable SFOAEs across most of the tested frequency range when measured with a 40 dB SPL probe.

The phase slope of the SFOAE was steeper and the normalized delay, N_{SFOAE}, was longer in middle-aged and older adults compared to young-adults. When changes with age are averaged across the five center frequencies, the data in Fig. 4 indicate that N_{SFOAE} increases by roughly 0.035 periods per year (cf., the mean slope $m_{N_{SFOAE}}$ in Table 1). The standing-wave model of spontaneous OAE generation (Shera 2003) predicts that increases in SFOAE phase slope produce decreases in the frequencies of spontaneous OAEs (SOAEs). Indeed, one can show that the expected fractional change in SOAE frequency per year is approximately $-m_{N_{SFOAE}}/N_{SFOAE}$. Evaluating this prediction using representative parameter values ($-m_{N_{SFOAE}} \sim 0.035$ periods/year and $N_{SFOAE} \sim 15$ periods) gives an estimated SOAE frequency shift of –0.24%/year, a value in close agreement with Burns (2017), who observed a near linear, downward frequency shift in spontaneous OAE frequency in a small group of human ears over seven decades of life, averaging –0.25% per year.

Because OAE delays have been linked to cochlear tuning (e.g., Shera et al. 2002, 2010), increases in SFOAE delay seem to suggest sharper tuning in aging adults. *Sharper* tuning curves in the elderly appear unlikely and difficult to explain. Both this seemingly paradoxical result and the counter-intuitive relative preservation of SFOAE levels during aging suggest that reflection emissions, although sensitive to cochlear gain, are influenced by additional factors that vary with age and whose effects may become especially salient in the elderly. Thus, reflection emissions in elderly ears may not gauge the same processes in the same way as they do in healthy young-adult ears. Just as SFOAE levels in aging ears do not correlate as well to the audiogram as DPOAE levels, SFOAE delays in older human ears may not correlate as well with tuning because they are influenced by additional factors linked to aging.

Although the mechanical changes that produce steeper phase gradients and longer SFOAE delays in aging ears remain unclear, longer delays are consistent with a decrease in the effective stiffness of the cochlear partition (Burns 2009, 2017). To account for the downward frequency shifts observed in SOAE frequencies, Burns hypothesized that the basilar membrane becomes more compliant with age. Because transverse waves generally propagate with a speed proportional to the square root of the effective stiffness (or restoring force) of the medium, declines in stiffness yield slower wave speeds, increased travel times, and longer delays. The longer SFOAE phase-gradient delays we observed in the aged are therefore consistent with a more compliant basilar membrane. Morphological studies of human temporal bones argue against substantial changes in basilar-membrane thickness with age, except at the very basal regions (Bhatt et al. 2001). However, the sensitivity of this one morphological feature to anything that might produce changes in stiffness is unclear. More nuanced features, such as the integrity of the collagen-containing radial fibers within the basilar membrane, are not accessible by light microscopy but may have a stronger link to function.

SFOAE Preservation and the Role of Increasing Roughness

The most compelling finding of the present study is that the SFOAE, an emission generated by cochlear reflection, does not show the same rate of decline with age as the DPOAE, an emission generated by cochlear nonlinearities. Additionally, we find that SFOAEs are less reliably correlated with hearing thresholds than distortion emissions in aged ears. When we re-analyzed the DPOAE component data of Abdala and Dhar (2012, see Fig. 7), we found patterns of relative component decline similar to those found here: the slope of the DPOAE distortion-component reduction with age (over a 48-year span) was roughly twice that of the reflection-component decline at both low (1 kHz) and high (4 kHz) frequencies. Our results here and those of the prior study support the idea that the natural aging process affects the generation of SFOAEs and DPOAEs differently. Age-related changes in the factors underlying SFOAE generation may make SFOAEs less sensitive to slight or mild hearing loss in the elderly. Reflection emissions, which arise near the peak of the traveling wave evoked by the probe tone, are thought to be sensitive to alterations in cochlear gain, also strongest near the peak. Study results have

shown that mild hearing losses do impact reflection emissions (e.g., click-evoked and stimulus-frequency OAEs) more significantly than they do distortion emissions, which are often measurable by standard protocols in subjects with even moderate degrees of hearing loss (Gorga et al. 1993, 1997; Lapsley-Miller et al. 2004; Abdala and Kalluri 2017). Aging may introduce additional factors that alter the established link between reflection OAEs and hearing sensitivity. In this study, when we eliminated aging (and any factor associated with aging) by analyzing only the data from subjects younger than 42 years, the level decline of the SFOAE and DPOAE with age (not aging) became similar.

Dong and Olson (2010) used a combination of intra-cochlear and OAE measurements from gerbil ear to study the source of DPOAEs. They found that local cochlear damage characteristically reduces distortion components within the damaged region but *increases* reflection-type components. Did the punctate local damage introduce irregularities that enhanced cochlear reflection more than it reduced the amplifier gain? In humans, the mild and relatively slow-onset tissue degradation associated with aging may produce a similar effect. Our results indicate that some factor (or factors) that differentially impacts SFOAE but not DPOAE generation is at play during aging. Modeling conducted with SFOAE simulations suggests that increasing irregularity with aging could be this factor.

The model of SFOAE generation indicates that for realistic parameter choices, SFOAE levels depend on three principal factors: round-trip middle-ear transmission [G_{ME} in Eq. (1)], traveling-wave gain ($\hat{W}$ in Eq. (3)), and the micromechanical roughness that scatters the wave [$\varepsilon(x)$ in Eq. (2)]. Because the first two factors also play key roles in determining DPOAE levels, we hypothesized that the third, micromechanical irregularity, provides a plausible source for the observed differential effect of aging on relative SFOAE and DPOAE levels. (Of course, some factor more strongly involved in DPOAE than in SFOAE generation may also contribute.) Since simulated SFOAE levels depend on the product of the roughness magnitude and the square of the cochlear gain [Eq. (2)], decreases in gain can be compensated for by increases in roughness. To explore this idea in the model, we used the correlation between DPOAE levels and hearing thresholds to estimate the cochlear gain parameter [Eq. (4)] as a function of hearing level. Then, by changing the roughness magnitude with age, we showed that the model can reproduce the observed relative preservation of SFOAE versus DPOAE levels. Our estimate of the necessary increase in roughness—a factor of 2–4 over the lifespan—depends inversely on our DPOAE-based estimate of cochlear gain and its variation with HL; for example, larger decreases in cochlear gain require correspondingly larger increases in roughness. At some point, of course, decreases in gain associated with presbycusis must drive measured SFOAE levels into the noise floor and cannot be compensated by biologically plausible increases in roughness.

Clinical Implications

The characteristic SFOAE–DPOAE pattern observed here during aging offers both a caution and promise. In aging ears, reflection OAEs may not be as sensitive an indicator of hearing loss as we believe them to be in young ears. There may be a healthy form of reflection (arising from the natural irregularity present in all ears) that predicts normal hearing, and a more pathological form arising from irregularities introduced by the aging process, that weakens this prediction. Unless both reflection- and distortion-source OAEs are assessed together, this type of cochlear deficit may not be identified, and an audiologist might underestimate the degree of hearing loss in elderly individuals who cannot reliably complete an audiogram.

The promise of this joint-OAE profile lies in differential diagnosis. Two elderly individuals of comparable age with similar audiograms may well have different underlying deficits or etiologies based on their different life courses and histories. Using a joint-OAE profile recorded serially as an individual ages, the signature pattern observed here might emerge and determine the etiology to be aging-related, which could impact the intervention. With the advent of gene therapies and hair-cell regeneration, correctly identifying the underlying pathologies associated with any given hearing loss will become critically important for understanding the success or failure of such therapies.

Other auditory pathologies, etiologies, and deficits may have their own signature joint SFOAE–DPOAE profiles that become evident with OAE monitoring during vocational noise exposure, for example, or ototoxic drug therapy. These profiles could allow audiologists to discriminate among mild-moderate hearing losses that have similar audiograms but different etiologies and corresponding perceptual difficulties. Discovering these diagnostic patterns will require a large-scale, longer-term study of the joint reflection and distortion OAE profile in individuals with sensory hearing losses of varied etiologies. A preliminary study with a small group of impaired ears has already shown the potential of such profiles to distinguish among ears with otherwise similar hearing (Abdala and Kalluri 2017). These profiles may explain variance in hearing and cochlear health that the audiogram has been unable to capture. It is hoped

that with a combined measurement of reflection and distortion OAEs we come to more fully understand the normal and the impaired cochlea in ways that enhance clinical diagnosis and intervention.

ACKNOWLEDGEMENTS

Supported by NIH/NIDCD Grants R01 DC003552 (C.A.) and R01 DC003687 (C.A.S.). We are grateful to Yeini Guardia for assistance in data collection and management and to Ping Luo for assistance in data analysis.

COMPLIANCE WITH ETHICAL STANDARDS

Conflict of Interest Statement

None of the authors of this research study have a commercial interest in this work nor other conflicts of interest.

REFERENCES

Abdala C, Dhar S (2010) Distortion product otoacoustic emission phase and component analysis in human newborns. J Acoust Soc Am 127:316–325

Abdala C, Dhar S (2012) Maturation and aging of the human cochlea: A view through the DPOAE looking glass. J Assoc Res Otolaryngol 13:403–421

Abdala C, Kalluri R (2017) Towards a joint reflection-distortion otoacoustic emission profile: results in normal and impaired ears. J Acoust Soc Am 142:812–824

Abdala C, Mishra SK, Williams TL (2009) Considering distortion product otoacoustic emission fine structure in measurements of the medial olivocochlear reflex. J Acoust Soc Am 125:1584–1594

Abdala C, Luo P, Shera CA (2015) Optimizing swept-tones to measure DPOAEs in adult and newborn ears. J Acoust Soc Am 138:3785–3799

Abdala C, Luo P, Shera CA (2016) Comparison of methods for DPOAE component separation. Poster presented to the 39th midwinter meeting of the Association for Research in Otolaryngology, San Diego, CA

Abdala C, Guardia Y, Luo P, Shera CA (2018) Swept-tone stimulus frequency otoacoustic emissions: Normative data and methodological considerations. J Acoust Soc Am 143:181–192

Bhatt K, Liberman MC, Nadol JB Jr (2001) Morphometric analysis of age-related changes in the human basilar membrane. Ann Otol Rhinol Laryngol 110:1147–1153

Burns EM (2009) Long-term stability of spontaneous otoacoustic emissions. J Acoust Soc Am 125:3166–3176

Burns EM (2017) Even longer term stability of spontaneous otoacoustic emissions. J Acoust Soc Am 142:1828–1831

Castor X, Veuillet E, Morgon A, Collet L (1994) Influence of aging on active cochlear micromechanical properties and on the medial olivocochlear system in humans. Hear Res 77:1–8

Cheatham M, Ahmad A, Zhou A, Goodyear Y, Dallos P, Richardson J (2016) Increased spontaneous otoacoustic emissions in mice with a detached tectorial membrane. J Acoust Soc Am 17:81–88

Deeter R, Abel R, Calandruccio L, Dhar S (2009) Contralateral acoustic stimulation alters the magnitude and phase of distortion product otoacoustic emissions. J Acoust Soc Am 126:2413–2424

Dong W, Olson ES (2010) Local cochlear damage reduces local nonlinearity and decreases generator-type cochlear emissions while increasing reflector-type emissions. J Acoust Soc Am 127:1422–1431

Dorn PA, Piskorski P, Keefe DH, Neely ST, Gorga MP (1998) On the existence of an age/threshold/frequency interaction in distortion product otoacoustic emissions. J Acoust Soc Am 104:964–971

Fitzgibbons PJ, Gordon-Salant S (2010) Behavioral studies with aging humans: Hearing sensitivity and psychoacoustics. In: Gordon-Salant S, Frisina RD, Fay RR, Popper AN (eds) The aging auditory system. Springer, New York, pp 111–134

Gorga MP, Neely ST, Bergman B, Beauchaine KL, Kaminski JR, Peters J, Jesteadt W (1993) Otoacoustic emissions from normal-hearing and hearing-impaired subjects: Distortion product responses. J Acoust Soc Am 93:2050–2060

Gorga MP, Neely ST, Ohlrich B, Hoover B, Redner J, Peters J (1997) From laboratory to clinic: A large-scale study of distortion product otoacoustic emissions in ears with normal hearing and ears with hearing loss. Ear Hear 18:440–455

Greenwood DD (1990) A cochlear frequency-position function for several species—29 years later. J Acoust Soc Am 87:2592–2605

Hopkins K, Moore BC (2011) The effects of age and cochlear hearing loss on temporal fine structure sensitivity, frequency selectivity, and speech reception in noise. J Acoust Soc Am 130:334–349

Hoth S, Gudmundsdottir K, Plinkert P (2010) Age dependence of otoacoustic emissions: the loss of amplitude is primarily caused by age-related hearing loss and not by aging alone. Eur Arch Otoryhinolaryngol 267:679–690

Kalluri R, Shera CA (2013) Measuring stimulus-frequency otoacoustic emissions using swept-tones. J Acoust Soc Am 134:356–368

Konrad-Martin D, Keefe DH (2005) Transient-evoked stimulus-frequency and distortion-product otoacoustic emissions in normal and impaired ears. J Acoust Soc Am 117:3799–3815

Kummer P, Janssen T, Hulin P, Arnold W (1998) The level and growth behavior of the $2f_1$–f_2 distortion product otoacoustic emission and its relationship to auditory sensitivity in normal hearing and cochlear hearing loss. J Acoust Soc Am 103:3431–3444

Lapsley-Miller JA, Marshall L, Heller LM (2004) A longitudinal study of changes in evoked otoacoustic emissions and pure-tone thresholds as measured in a hearing conservation program. Int J Audiol 43:307–322

Lee J, Dhar S, Abel R, Banakis R, Grolley E, Lee J, Zecker S, Siegel J (2012) Behavioral hearing thresholds between 0.125 and 20 kHz using depth-compensated ear simulator calibration. Ear Hear 33:315–329

Long GR, Talmadge CL, Lee J (2008) Measuring distortion product otoacoustic emissions using continuously sweeping primaries. J Acoust Soc Am 124:1613–1626

Lonsbury-Martin BL, Cutler WM, Martin GK (1991) Evidence for the influence of aging on distortion-product otoacoustic emissions in humans. J Acoust Soc Am 89:1749–1759

Mishra SK, Biswal M (2016) Time–frequency decomposition of click evoked otoacoustic emissions in children. Hear Res 335:161–178

Moleti A, Longo F, Sisto R (2012) Time-frequency domain filtering of evoked otoacoustic emissions. J Acoust Soc Am 132:2455–2467

Morrell CH, Gordon-Salant S, Pearson JD, Brant LJ, Fozard JL (1996) Age- and gender-specific reference ranges for hearing level and longitudinal changes in hearing level. J Acoust Soc Am 100:1949–1967

Ortmann AJ, Abdala C (2016) Changes in the compressive nonlinearity of the cochlea during early aging: estimates from distortion OAE input/output functions. Ear Hear 37:603–614

Ortmann AJ, Guardia YC, Abdala C (2017) Aging and cochlear nonlinearity as measured with distortion OAEs and loudness

perception. Poster presented to the 40th Annual Midwinter Meeting of the Assoc Res Otolaryngol, Baltimore, MD

POLING GL, SIEGEL JH, LEE J, LEE J, DHAR S (2014) Characteristics of the $2f(_1)$–$f(_2)$ distortion product otoacoustic emission in a normal hearing population. J Acoust Soc Am 135:287–299

RAO A, LONG GR (2011) Effects of aspirin on distortion product fine structure: interpreted by the two-source model for distortion product otoacoustic emissions generation. J Acoust Soc Am 129:792–800

SATOH Y, KANZAKI J, O-UCHI T, YOSHIHARA S (1998) Age-related changes in transiently evoked otoacoustic emissions and distortion product otoacoustic emissions in normal-hearing ears. Auris Nasus Larynx 25:121–130

SCHAIRER KS, FITZPATRICK DH, KEEFE DH (2003) Input–output functions for stimulus-frequency otoacoustic emissions in normal-hearing adult ears. J Acoust Soc Am 114:944–966

SHERA CA (2003) Mammalian spontaneous otoacoustic emissions are amplitude-stabilized cochlear standing waves. J Acoust Soc Am 114:244–262

SHERA CA, BERGEVIN C (2012) Obtaining reliable phase-gradient delays from otoacoustic emissions data. J Acoust Soc Am 132:927–943

SHERA CA, GUINAN JJ (1999) Evoked otoacoustic emissions arise by two fundamentally different mechanisms: A taxonomy for mammalian OAEs. J Acoust Soc Am 105:782–798

SHERA CA, GUINAN JJ (2003) Stimulus-frequency-emission group delay: A test of coherent reflection filtering and a window on cochlear tuning. J Acoust Soc Am 113:2762–2772

SHERA CA, GUINAN JJ, OXENHAM AJ (2002) Revised estimates of human cochlear tuning from otoacoustic and behavioral measurements. Proc Natl Acad Sci U S A 99:3318–2232

SHERA CA, TUBIS A, TALMADGE CL (2005) Coherent reflection in a two-dimensional cochlea: Short-wave versus long-wave scattering in the generation of reflection-source otoacoustic emissions. J Acoust Soc Am 118:287–313

SHERA CA, TUBIS A, TALMADGE CL (2008) Testing coherent reflection in chinchilla: Auditory-nerve responses predict stimulus-frequency emissions. J Acoust Soc Am 124:381–395

SHERA CA, GUINAN JJ, OXENHAM AJ (2010) Otoacoustic estimation of cochlear tuning: Validation in the chinchilla. J Assoc Res Otolaryngol 11:343–365

STOVER L, NORTON S (1993) The effects of aging on otoacoustic emissions. J Acoust Soc Am 94:2670–2681

TALMADGE CL, TUBIS A, LONG GR, TONG C (2000) Modeling the combined effects of basilar membrane nonlinearity and roughness on stimulus frequency otoacoustic emission fine structure. J Acoust Soc Am 108:2911–2932

UCHIDA Y, ANDO F, SHIMOKATA H, SUGIURA S, UEDA H, NAKASHIMA T (2008) The effects of aging on distortion-product otoacoustic emissions in adults with normal hearing. Ear Hear 29:176–184

WHITEHEAD ML, STAGNER BB, MARTIN GK, LONSBURY-MARTIN BL (1996) Visualization of the onset of distortion-product otoacoustic emissions, and measurement of their latency. J Acoust Soc Am 100:1663–1679

ZWEIG G, SHERA CA (1995) The origin of periodicity in the spectrum of evoked otoacoustic emissions. J Acoust Soc Am 98:2018–2047